

# In Vitro Anticancer Drug Sensitivity Sensing through Single-Cell Raman Spectroscopy

Jingkai Wang <sup>1,2</sup>, Kaicheng Lin <sup>2</sup>, Huijie Hu <sup>1,2</sup>, Xingwang Qie <sup>2</sup>, Wei E. Huang <sup>3</sup>, Zhisong Cui <sup>4,5,\*</sup>, Yan Gong <sup>2,\*</sup> and Yizhi Song <sup>2,\*</sup>

<sup>1</sup> School of Biomedical Engineering (Suzhou), Division of Life Sciences and Medicine, University of Science and Technology of China, Hefei 230026, China; wangjk@sibet.ac.cn (J.W.); huhj@sibet.ac.cn (H.H.)

<sup>2</sup> Suzhou Institute of Biomedical Engineering and Technology, Chinese Academy of Sciences, Suzhou 215163, China; linkc@sibet.ac.cn (K.L.); qiexw@sibet.ac.cn (X.Q.)

<sup>3</sup> Department of Engineering Science, University of Oxford, Parks Road, Oxford OX1 3PJ, UK; wei.huang@eng.ox.ac.uk

<sup>4</sup> Marine Bioresources and Environment Research Center, First Institute of Oceanography, Ministry of Natural Resources of China, Qingdao 266061, China

<sup>5</sup> Laboratory for Marine Ecology and Environmental Science, Qingdao National Laboratory for Marine Science and Technology, Qingdao 266071, China

\* Correspondence: czs@fio.org.cn (Z.C.); gongy@sibet.ac.cn (Y.G.); songyz@sibet.ac.cn (Y.S.)

## 1. Materials and Methods

### 1.1. The setup of a Raman microscopy sensing system

The confocal Raman spectrometer was assembled based on an Olympus upright microscope (BX43F, Olympus, Tokyo, Japan). A detailed system schematic of the home-built confocal Raman spectrometer is shown in Figure S1. In addition, the specifications of the system are listed in Table S1.

**Citation:** Wang, J.; Lin, K.; Hu, H.; Qie, X.; Huang, W.E.; Cui, Z.; Gong, Y.; Song, Y. In Vitro Anticancer Drug Sensitivity Sensing through Single-Cell Raman Spectroscopy. *Biosensors* **2021**, *11*, 286. <https://doi.org/10.3390/bios11080286>

Received: 16 July 2021

Accepted: 17 August 2021

Published: 20 August 2021

**Publisher's Note:** MDPI stays neutral with regard to jurisdictional claims in published maps and institutional affiliations.



**Copyright:** © 2021 by the author. Licensee MDPI, Basel, Switzerland. This article is an open access article distributed under the terms and conditions of the Creative Commons Attribution (CC BY) license (<http://creativecommons.org/licenses/by/4.0/>).

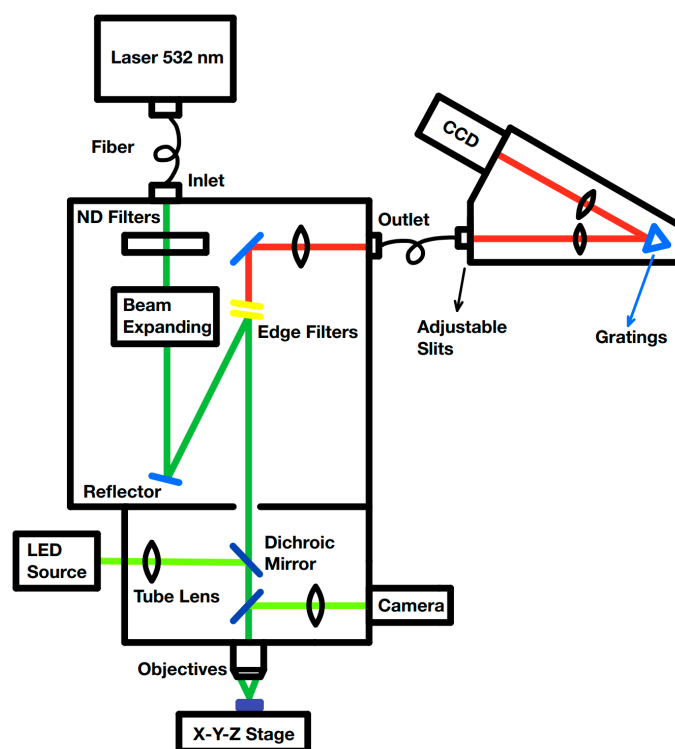


**Figure S1.** Detailed system schematic of the home-built confocal Raman spectrometer. ND Filters: Neutral Density Filters. The laser, confocal microscopy module, and spectrometer are connected via fibers.

**Table S1.** The specifications of the confocal Raman spectrometer.

Module	Specifications	Value	Condition
Confocal Microscopy Module	X-Y space resolution	Better than 500 nm	100× NA0.95 objective
	Z space resolution	Better than 900 nm	100× NA0.95 objective
Spectrometer Module	Spectral resolution	3 cm <sup>-1</sup>	600 lines/mm grating
	Spectral range	400-3400 cm <sup>-1</sup>	

### 1.2. Data analysis

There are several terms that are commonly used along with the description of sensitivity, specificity and accuracy. They are true positive (TP), true negative, false negative (FN), and false positive (FP) [1].

Sensitivity, specificity and accuracy are described in terms of TP, TN, FN and FP.

Sensitivity =  $TP/(TP + FN)$  = (Number of true positive assessments)/(Number of all positive assessments)

Specificity =  $TN/(TN + FP)$  = (Number of true negative assessments)/(Number of all negative assessments)

Accuracy =  $(TN + TP)/(TN + TP + FN + FP)$  = (Number of correct assessments)/Number of all assessments

## 2. Results and Discussion

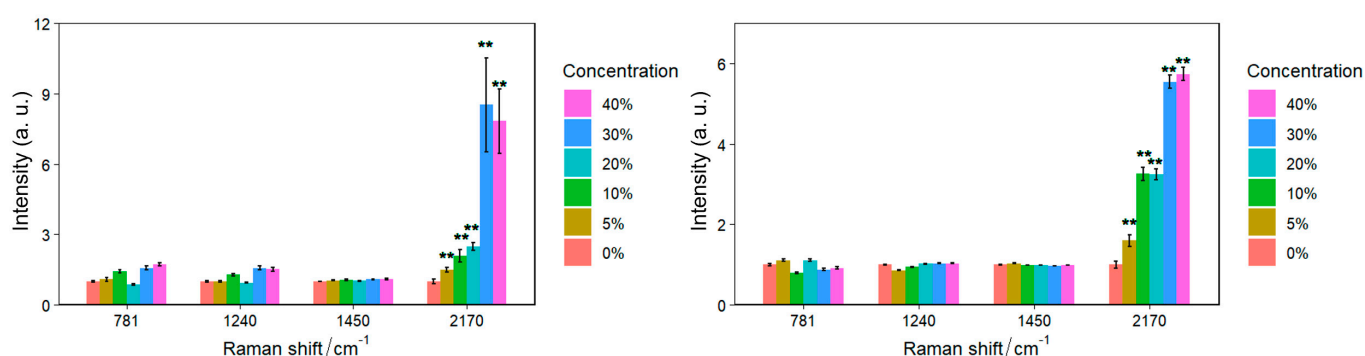


**Figure S2.** Changes in Raman intensities for nucleic acid (781 cm<sup>-1</sup>), protein (1240 cm<sup>-1</sup>), protein and lipids (1450 cm<sup>-1</sup>), and carbon-deuterium bond (2170 cm<sup>-1</sup>) of HCC827(A) and MCF-7 (B) cell lines under different D<sub>2</sub>O concentrations. The intensity of all peaks in negative control (0% D<sub>2</sub>O) was normalized. Bars represent the average intensity (n ≥ 100). \*\*: p ≤ 0.01; intensities at other positions show no significant difference. The error bars represent the standard error.

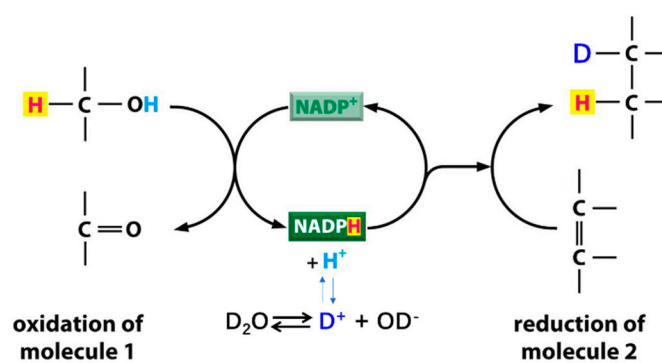


Figure S3. Illustration of deuterium from D<sub>2</sub>O incorporation to biomolecules by active cells.

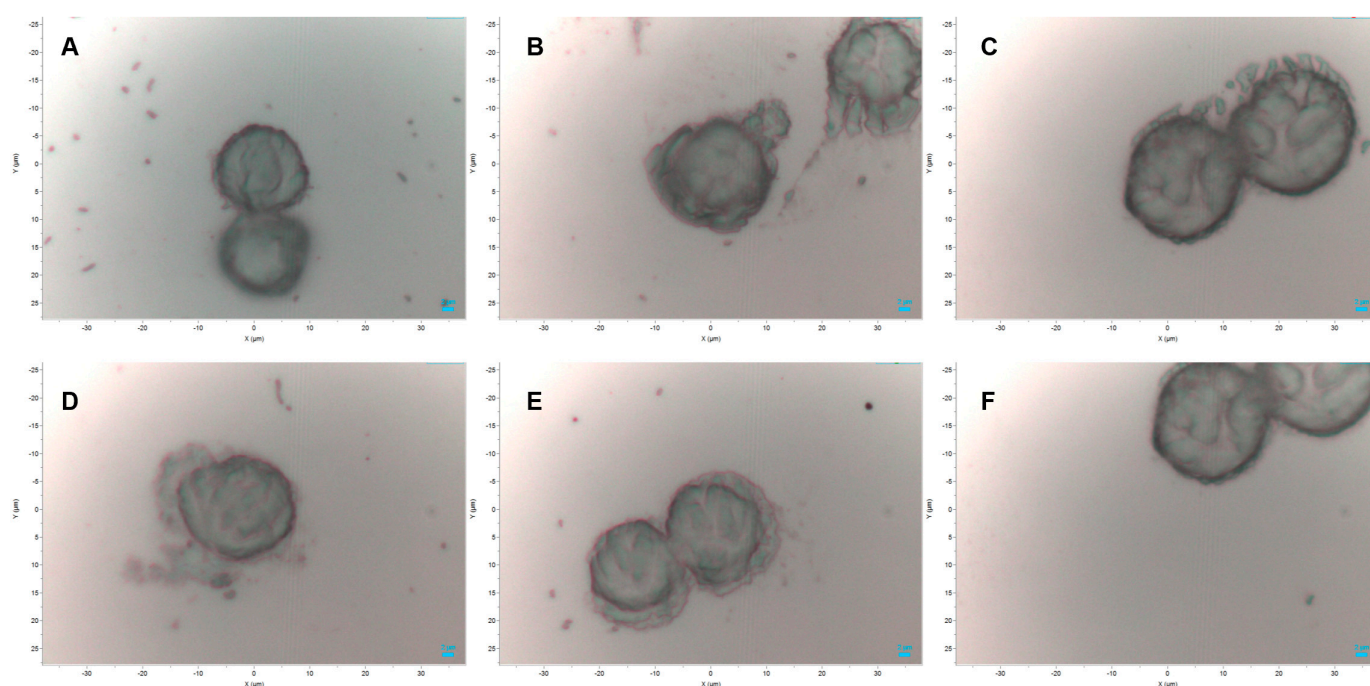
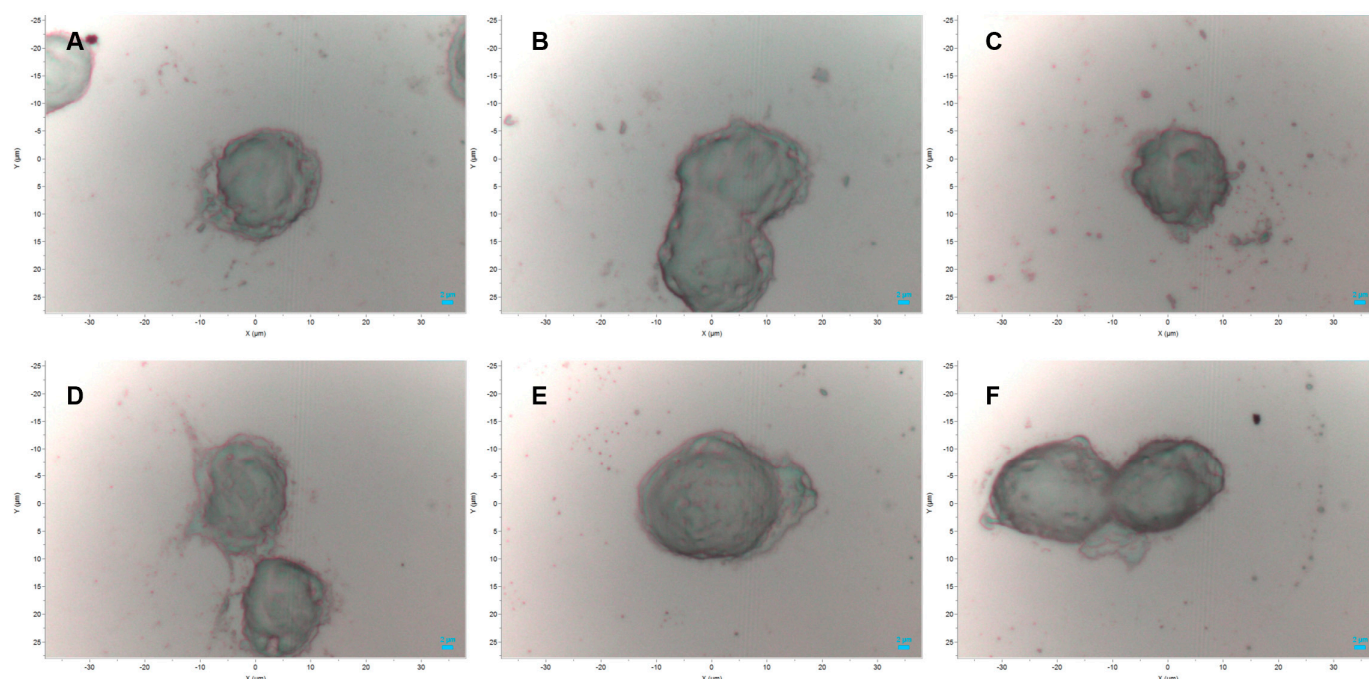


Figure S4. Bright-field microscopic images (50× objective) MCF-7 cells treated with D<sub>2</sub>O for 12 h. Cells were fixed by 4% paraformaldehyde and transferred to aluminum slide and air-dried. The concentration of D<sub>2</sub>O was (A) 0%, (B) 5%, (C) 10%, (D) 20%, (E) 30%, (F) 40%. The scale bars represent 2 μm.



**Figure S5.** Bright-field microscopic images (50× objective) MCF-7 cells treated with D<sub>2</sub>O for 36 h. Cells were fixed by 4% paraformaldehyde and transferred to aluminum slide and air-dried. The concentration of D<sub>2</sub>O was (A) 0%, (B) 5%, (C) 10%, (D) 20%, (E) 30%, (F) 40%. The scale bars represent 2 µm.

**Table S2.** The difference of viability of cancer cells at different D<sub>2</sub>O/H<sub>2</sub>O concentrations.

<i>Group condition</i>	<i>Sample species</i>	<i>P value</i>	<i>Significance</i>
10% D <sub>2</sub> O	HCC827	0.09081	No significance
	MCF-7	0.38674	No significance
20% D <sub>2</sub> O	HCC827	0.35162	No significance
	MCF-7	0.38310	No significance
30% D <sub>2</sub> O	HCC827	0.41138	No significance
	MCF-7	0.19432	No significance
40% D <sub>2</sub> O	HCC827	0.31447	No significance
	MCF-7	0.02608	*

\*: p < 0.05; No significance: p > 0.05

**Table S3.** IC<sub>20</sub>, IC<sub>30</sub>, IC<sub>40</sub>, and IC<sub>50</sub> (µM) of different chemotherapy drugs.

<i>Cell lines</i>	<i>Drugs</i>	<i>IC<sub>50</sub> of population level analysis (µM)</i>	<i>Correlation coefficient (r)</i>	<i>IC<sub>20</sub> of single-cell Raman-DIP (µM)</i>	<i>IC<sub>30</sub> of single-cell Raman-DIP (µM)</i>	<i>IC<sub>40</sub> of single-cell Raman-DIP (µM)</i>	<i>Correlation coefficient (r)</i>
HCC827	Afatinib	0.0013	0.974	0.0020	0.0032	0.0049	0.963
	Cisplatin	12.56	0.976	4.68	10.35	>100	0.994
	Crizotinib	1.59	0.997	2.82	6.54	>30	0.975
	Gefitinib	0.015	0.994	0.0046	0.0082	0.014	0.899
	Icotinib	0.041	0.995	0.034	0.076	0.16	0.995

	Osimertinib	0.011	0.995	0.0065	0.010	0.016	0.910
	Cisplatin	15.67	0.999	11.56	20.10	37.63	0.985
MCF-7	Gemcitabine	>30	0.906	2.62	>30	>30	0.803
	MMAE	$6.33 \times 10^{-5}$	0.981	$2.06 \times 10^{-4}$	$4.29 \times 10^{-4}$	>0.1	0.854

To choose the most appropriate criterion for evaluating drug efficacy at the single-cell level, we calculated the sensitivity, specificity and accuracy of IC<sub>20</sub>, IC<sub>30</sub>, and IC<sub>40</sub>. In the population level IC<sub>50</sub> of the drugs, 10 µM serves as the benchmark for the chemotherapy drugs to evaluate their efficacy. Similar to the IC<sub>50</sub>, the drug resistance results at single-cell level are summarized in Table S4. Of the three ICs, we chose IC<sub>30</sub> as the final criterion for the single-cell Raman-DIP approach because it had the best sensitivity, specificity, and accuracy.

**Table S4.** Sensitivity, specificity, and accuracy of the criteria IC<sub>20</sub>, IC<sub>30</sub>, and IC<sub>40</sub>.

Cell lines	Drugs	IC <sub>50</sub> of population level analysis	IC <sub>20</sub> of single-cell Raman-DIP	IC <sub>30</sub> of single-cell Raman-DIP	IC <sub>40</sub> of single-cell Raman-DIP
HCC827	Afatinib	S	S (TP)	S (TP)	S (TP)
	Cisplatin	R	S (FP)	R (TN)	R (TN)
	Crizotinib	S	S (TP)	S (TP)	R (FN)
	Gefitinib	S	S (TP)	S (TP)	S (TP)
	Icotinib	S	S (TP)	S (TP)	S (TP)
	Osimertinib	S	S (TP)	S (TP)	S (TP)
MCF-7	Cisplatin	R	R (TN)	R (TN)	R (TN)
	Gemcitabine	R	S (FP)	R (TN)	R (TN)
	MMAE	S	S (TP)	S (TP)	S (TP)
	Sensitivity		1.0	1.0	0.83
	Specificity		0.33	1.0	1.0
	Accuracy		0.78	1.0	0.89

R: Resistant, S: Sensitive. TP: true positive, TN: true negative, FN: false negative, and FP: false positive.

## References

1. Zhu, W., N. Zeng, and N. Wang, *Sensitivity, Specificity, Accuracy, Associated Confidence Interval and ROC Analysis with Practical SAS® Implementations*. NorthEast SAS users group, health care and life sciences, 2010.